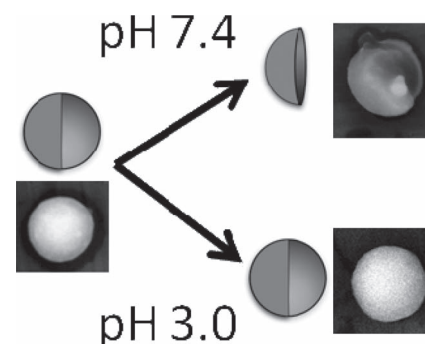


Differentially Degradable Janus Particles for Controlled Release Applications

Sangyeul Hwang, Joerg Lahann*

Janus particles with differentially degradable compartments were prepared by electrohydrodynamic (EHD) co-jetting and subsequent controlled crosslinking. These bicompartamental particles are composed of an interpenetrating polymer network of poly(ethylene oxide) and poly(acrylamide-co-acrylic acid) in one hemisphere and a crosslinked copolymer of dextran and poly(acrylamide-co-acrylic acid) segments in the second compartment. The compositional anisotropy caused differential hydrolytic susceptibility: Although both compartments were stable at pH 3.0, selective degradation of the PEO-containing compartment at pH 7.4 was observed within 5 days. Janus particles with differentially degradable polymer compartments may be of interest for a range of oral drug delivery applications because of their propensity for decoupled release profiles.



1. Introduction

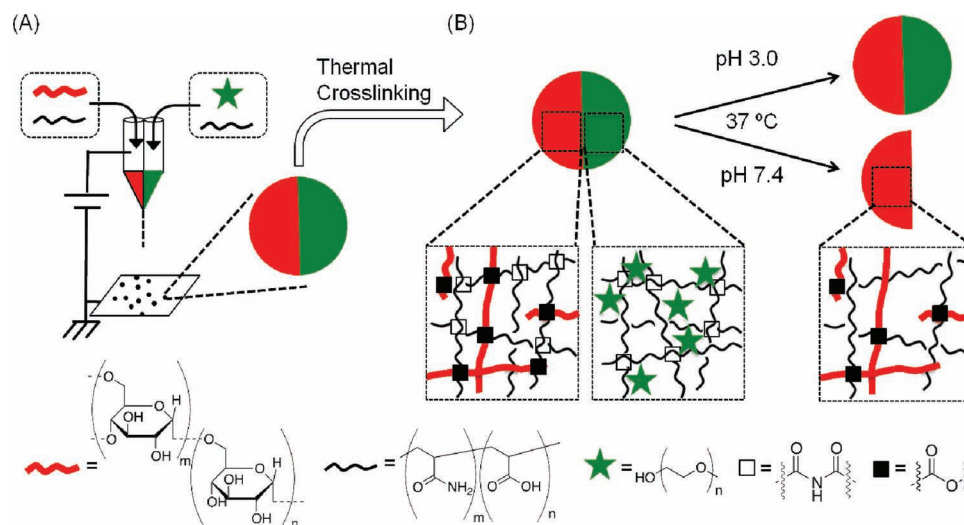
Multifunctionality is a key feature of anisotropic polymer particles that are composed of two or more different compartments.^[1] In recent years, a number of Janus-type micro- and nanoparticles have been reported.^[2,3] For example, amphiphilic surface patterning in Janus particles resulted in unique particle assemblies, such as triple helices^[4] or colloidal kagome lattices.^[5] Self-propellant metal Janus particles can convert chemical fuels into directed motion,^[6,7] and regiospecific binding of Janus particles has been used for unidirectional targeting of cell surface receptors in an attempt to create biohybrid materials.^[8] Thus, anisotropic particles are pertinent to a number of scientific areas including self-assembly,^[4,5,9,10] self-propulsion,^[6,7,11] display,^[12,13] biological applications,^[8,14] and analytical probes.^[15,16]

Anisotropic particles can be broadly grouped into two types; surface patterned “patchy” particles and bulk anisotropic “compartmentalized” particles. Metal deposition^[4,17] and nanoparticle lithography^[18] are effective strategies for fabricating patchy particles. Microfluidic techniques^[12,19] and electrohydrodynamic (EHD) co-jetting^[20] are representative approaches for manufacturing compartmentalized particles. In particular, EHD co-jetting has been remarkably versatile for the preparation of multicompartamental anisotropic particles.^[21–26] For example, inorganic materials such as gold,^[26] magnetite,^[25] and titanium dioxide^[25] were selectively embedded in defined compartments. Janus particles with different polymer compositions in each compartment were also prepared using this approach.^[24]

By taking advantages of EHD co-jetting for combining dissimilar materials within the same particle, preparation of differentially degradable multi-compartmentalized particles becomes plausible. Moreover, if the differential degradation can be triggered by an appropriately controlled stimulus, such as a change in pH value, new routes of oral administration of drugs may be developed.

Herein, a new type of stimuli-sensitive Janus particles is reported that allows for selective, pH-dependent

Dr. S. Hwang, Prof. J. Lahann
Departments of Chemical Engineering, Macromolecular
Science and Engineering, Materials Science and Engineering,
and Biomedical Engineering, University of Michigan, Ann
Arbor, MI 48109, USA
E-mail: lahann@umich.edu E-mail: lahann@umich.edu



Scheme 1. (A) Schematic description of the electrohydrodynamic (EHD) co-jetting process used to prepare bicompartmental Janus particles based on two different polymer solutions in DI water: one solution contains a poly(acrylamide-co-acrylic acid), (p(AAm-co-AA), 5.0 wt/v%), dextran (0.5 wt/v%), and RITC-dextran (0.5 wt/v%), the other has the copolymer (4.0 wt/v%), PEO (1.5 wt/v%), and FITC-PEO (0.5 wt/v%). (B) After thermal crosslinking at 175 °C, two different chemical bonds (imide vs. ester bonds) formed in the particle and give rise to different degradation rates for the two hemispheres.

degradation of individual compartments. That is, both compartments initially maintain stability at a lower pH (3.0), but only one compartment degrades at physiological pH after a defined time (Scheme 1). Therefore, we envision potential applications of these selectively degradable Janus particles for staged drug delivery.

2. Experimental Section

2.1. Materials

Poly(ethylene oxide) (PEO, 100 kDa), dextran (70 kDa), rhodamine B isothiocyanate conjugated dextran (RITC-dextran, $\bar{M}_w = 70$ kDa), fluorescein isothiocyanate (FITC), methylene chloride (CH_2Cl_2), and citric acid were products of Sigma-Aldrich Inc. (St. Louis, Missouri). Sodium dihydrogen phosphate monohydrate ($\text{NaH}_2\text{PO}_4 \cdot \text{H}_2\text{O}$) and sodium hydrogen phosphate heptahydrate ($\text{Na}_2\text{HPO}_4 \cdot 7\text{H}_2\text{O}$) were purchased from Fisher-Scientific Inc. (Pittsburgh, PA, USA). Poly(acrylamide-co-acrylic acid, sodium salts), P(AAm-co-AA) ($\bar{M}_w = 200$ kDa, 10% acrylic acids) was purchased from Polysciences Inc. (Warrington, PA, USA). All chemicals were used as received. The synthesis of FITC-conjugated PEO (FITC-PEO) was adapted from a published procedure.^[27] In brief, a mixture of FITC (0.2 g) and PEO (10 g) in CH_2Cl_2 (500 ml) was heated for 6 days under Ar atmosphere. After solvent removal, the residual solid was diluted in DI water, and dialyzed using a membrane filter (MWCO: 12–14 kDa; Spectrumlabs, Rancho Dominguez, CA, USA) to remove residual dye.

2.2. Electrohydrodynamic (EHD) Co-jetting

For EHD co-jetting, two jetting solutions were separately loaded in 1 mL syringes (Becton-Dickinson, Franklin Lakes, NJ, USA) and

were connected to a dual channel tip (FibriJet SA-3610; Micro-medics Inc., Eagan, MN, USA) with 26 gauge and 3.25 inch in length. The two polymer solutions were prepared as follows: (1) 5 wt/v% of p(AAm-co-AA), 0.5 wt/v% of dextran, and 0.5 wt/v% of RITC-dextran were dissolved in DI water; (2) 4 wt/v% of the copolymer, 1.5 wt/v% of PEO, and 0.5 wt/v% of FITC-PEO were combined in an aqueous solution. The two solutions were simultaneously controlled by a syringe pump (KD Scientific, USA) at a flow rate of 0.2 mL h⁻¹. The cathode of the high-voltage supply (Gamma High Voltage Research, Ormond Beach, FL, USA) was attached to the needle, and the ground was connected to the collecting substrate of aluminum foil (Fisher-Scientific Inc., Pittsburgh, PA, USA). Electrical DC potential of 15–18 kV was applied during the EHD co-jetting and the distance between the end of tip and the collecting substrate was 28–30 cm. All EHD co-jetting experiments were performed under ambient conditions. After jetting, the polymer particles were placed into an oven at a temperature of 175 °C for 3 h for chemical crosslinking.

2.3. Characterization

Confocal laser scanning microscopy (Leica, USA) was used to analyze the compartmentalization of the particles suspended in DI water (measured to be pH 6.5) after filtered and washed in DI water. An Ar/ArKr laser ($\lambda = 488$ nm) was used to excite FITC-PEO, and its emission window was set at 510–525 nm. A He-Ne laser ($\lambda = 543$ nm) was used to excite RITC-dextran, and the fluorescence emission was 580–595 nm. To confirm compartmentalized degradation of the Janus particles at different pH values and degradation times, all images were obtained under identical conditions including identical magnification, microscope settings, and laser powers. Superimposed images were obtained as overlays of two different fluorescence channels. Crosslinked particles were washed with DI water and placed on Al foil for subsequent

scanning electron microscopy (SEM; Nova Nanolab DulBeam, FEI corp., USA). For IR analysis, several gold-coated substrates were positioned on the top of Al foils prior to EHD co-jetting. The collected particles on the gold-coated substrates were placed into an oven at 175 °C at various time intervals (0–18 h) and analyzed using a Nicolet 6700 FT-IR spectrometer (Thermo Electron Corp., USA).

Particles were dispersed in either phosphate-citrate buffer (100×10^{-3} M, pH 3.0) or phosphate buffer (100×10^{-3} M, pH 7.4) for measurements of dynamic light scattering (DLS; ZEN3600, Malvern Instruments Ltd., UK) at the different pH values. All solutions were prepared from water purified using a Milli-RO/Milli-Q filtration system and filtered through a Millex-GS 0.22 μ m filter (Millipore, Bedford, MA). Particles (≈ 0.3 mg mL⁻¹) were dispersed in either phosphate-citrate buffer (100×10^{-3} M, pH 3.0) or phosphate buffer (100×10^{-3} M, pH 7.4). The specimen was allowed to equilibrate for 10 min and measured at an angle of 90° and room temperature.

2.4. Release Kinetics

To compare release at two different pH values, crosslinked particles (3.1 mg) were incubated in 1.5 mL of either phosphate-citrate buffer; (pH, 3.0) or phosphate buffer (pH, 7.4). The different particle suspensions were stirred at 37 °C and 0.2 mL of the sample was collected after a given period of time for further analysis (0, 1, 4, 9, 17, 48, and 100 h). Each portion was diluted in 2 mL of the phosphate buffer (pH, 7.4) and analyzed by UV spectroscopy (BioMates 3S, Thermo Scientific Inc., USA). Prior to the analysis, the absorbance values of a series of known concentrations of FITC-PEO were measured at $\lambda_{\text{max}}(\text{FITC-PEO}) = 491$ nm to obtain a FITC-PEO standard curve (see Figure S1, Supporting Information). Total released amount of FITC-PEO was then determined on the basis of this standard curve.

3. Results and Discussion

The EHD co-jetting technology has been shown to yield various types of multicompartmental polymer particles.^[20–26,28] EHD co-jetting can be performed with both organic solvents^[23,24,28] and water-based polymer solutions.^[20–22,25,26] Building on our earlier work,^[22,25,26] we pursued water-based jetting to produce submicron-sized polymer particles. The previous studies showed that once a water-soluble copolymer, p(AAm-co-AA), was electrosprayed and thermally heated at 175 °C, the particles were crosslinked via imide bond formation. After thermal crosslinking, the particles were fairly stable in water.^[22,25,26] For this purpose, we identified a new set of polymer compositions and chemistries for the two compartments. Compared with a previous study,^[22] increasing the content of dextran and adding PEO enabled manufacturing of pH-responsive degradable Janus particles. First, one of two jetting solutions contained 5 wt/v% of p(AAm-co-AA)(200 kDa, 10% AA), 0.5 wt/v% of dextran (70 kDa), and 0.5 wt/v% of rhodamine B isothiocyanate conjugated dextran (RITC-dextran, 70 kDa). This

polymer composition is corresponding to 83.3 wt% of the copolymer and 16.7 wt% of dextran after crosslinking at 175 °C. In this chemical crosslinking process, the copolymer forms imide bonds, whereas the dextran and copolymer copolymer are crosslinked via ester bonds (see Scheme 1B). The second jetting solution contained 4 wt/v% of the copolymer, 1.5 wt/v% of PEO (100 kDa), and 0.5 wt/v% of fluorescein isothiocyanate conjugated PEO (FITC-PEO, ≈ 100 kDa). This compartment will have 66.7 wt% the copolymer and 33.3 wt% PEO after thermally crosslinked. Thus, this compartment will be composed of an interpenetrating polymer network (IPN) where PEO chains will be physically entangled within the crosslinked copolymer (see Scheme 1 B). The distinctive polymer compositions and type of polymer networks of the two compartments will ultimately give rise to different degradation kinetics at physiological pH values. Fluorophores that were added into the two solutions to visualize the particles' compartmentalization can be also used as drug surrogates in subsequent release studies.

During thermal treatment of the Janus particles, carboxylic acid, hydroxyl, and amide groups can undergo chemical crosslinking. Both amide and carboxylic acid groups of the p(AAm-co-AA) can engage in imide bonds at elevated temperatures.^[22,25] In addition, amide and carboxylic acid groups of the copolymer as well as the imide bonds can eventually form ester bonds with free hydroxyl moieties of the dextran at the high temperature.^[29] After thermal crosslinking, infrared spectroscopy revealed the appearance of characteristic bands for imide groups at 1716 and 1219 cm⁻¹, whereas the N–H and O–H stretching bands as well as the C–O stretching band at 1113 cm⁻¹ were decreased, in addition to broadening of carbonyl stretching band in a region of 1670–1690 cm⁻¹ (Figure 1A). After thermal crosslinking for 3 h, the compartment composed of the IPN of PEO and p(AAm-co-AA) is stabilized only by imide bonds. Because the imide bonds are susceptible to hydrolysis at pH 7, the PEO-containing compartment can be slowly degradable at physiological pH and temperature. We note that direct esterification of end-standing hydroxyl groups in the PEO with ester groups in the p(AAm-co-AA) is in principle possible but can be neglected because of the low concentration of free hydroxyl groups. In contrast, the other compartment that contains the copolymer and dextran undergo chemical crosslinking imidation and esterification, where the ester bonds govern the hydrolytic stability for a longer time (Scheme 1B). In this formulation, the subtle balance of different chemical net points yields significantly different degradation rates for both compartments.

The maintenance of a well-defined compartmentalization after thermal crosslinking is a prerequisite for subsequent differential degradation studies. Compartmentalization after thermal crosslinking was confirmed

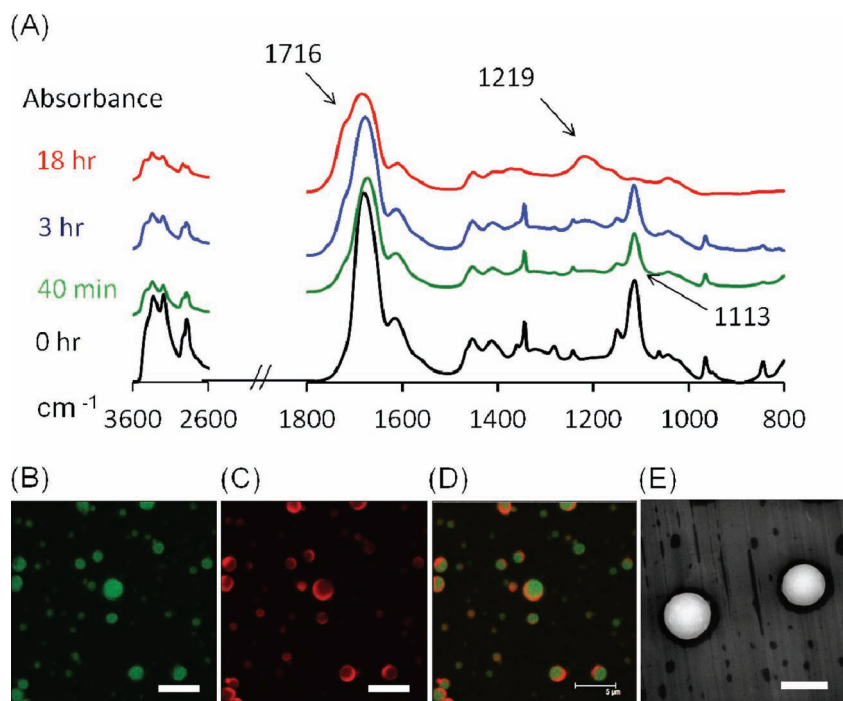


Figure 1. (A) Attenuated total reflectance (ATR) IR spectroscopy of Janus particles before and after thermal crosslinking. (B–D) Confocal Laser Scanning Microscopy (CLSM) micrographs of particles prepared via EHD co-jetting and thermal crosslinking at 175 °C; (B) a micrograph from a FITC channel, (C) a micrograph from a rhodamine channel, and (D) a superimposed image of (B) and (C) (see Experimental for details). (E) Scanning Electron Microscope (SEM) picture of these particles (10 kV and 25 000 × magnification). The scale bars are 5.00 μm in (B–D) and 1.0 μm in (E).

using confocal laser scanning microscopy (CLSM) (see Figure 1B–E), which compare well with similar types of compartmentalized particles reported in the literature.^[8,20–25,28,30] Here, the compositionally anisotropic particles featured the green color of the PEO compartment (FITC-PEO, Figure 1B) as well as the red color of the

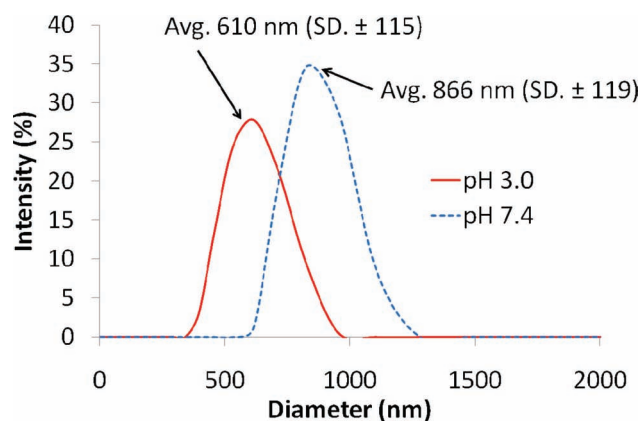


Figure 2. Dynamic light scattering (DLS; ZEN3600, Malvern Instruments Ltd., UK) was used to measure the average particle sizes at two different pH values (3.0 and 7.4), exhibiting that the particles are swelling at a higher pH.

dextran compartment (FITC-dextran, Figure 1C). The overlay of both fluorescent images confirms the bicompartamental architecture of the particles (Figure 1D). The spherical shape of particles is also shown by scanning electron microscopy (SEM, Figure 1E). Taken together, these results reinforce that the EHD co-jetting is in fact a suitable process to produce bicompartamental particles composed of two different types of crosslinked polymers.

Notably, carboxylated hydrogels, such as p(AAm-co-AA), are known to shrink in water at a low pH (<4), but swell at a higher pH (> 5) due to deprotonation of carboxylic acid groups (Figure S2, Supporting Information).^[30,31] Dynamic light scattering measurements of the particle dispersions at two different pH values, that is, pH 3.0 and 7.4 revealed that average particle diameter at pH 7.4 (866 ± 119 nm) was larger than the case of pH 3.0 (610 ± 115 nm) (see Figure 2). To evaluate degradation kinetics of the particles at pH 3.0 and 7.4, the particles were incubated at 37 °C in aqueous phosphate buffer solutions. A small portion of each suspension was collected at given time intervals and analyzed by UV spectroscopy to measure the released of FITC-PEO. The results are plotted in Figure 3. Here, the data were normalized to compare two series of experiments. At pH 3.0, which mimics the pH of the human stomach,^[32] The FITC-PEO release reached a plateau at about 30% after 3 days. However, at physiological

values and analyzed by UV spectroscopy to measure the released of FITC-PEO. The results are plotted in Figure 3. Here, the data were normalized to compare two series of experiments. At pH 3.0, which mimics the pH of the human stomach,^[32] The FITC-PEO release reached a plateau at about 30% after 3 days. However, at physiological

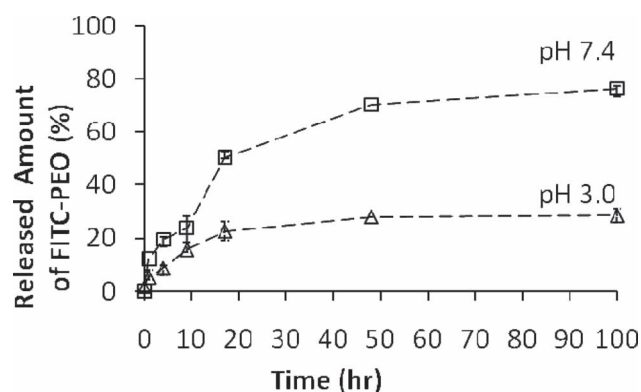


Figure 3. Normalized release profiles of FITC-PEO from the Janus particles at different pHs (pH 7.4, □; pH 3.0, Δ) at 37 °C, obtained by UV spectroscopy (see Experimental Section for details).

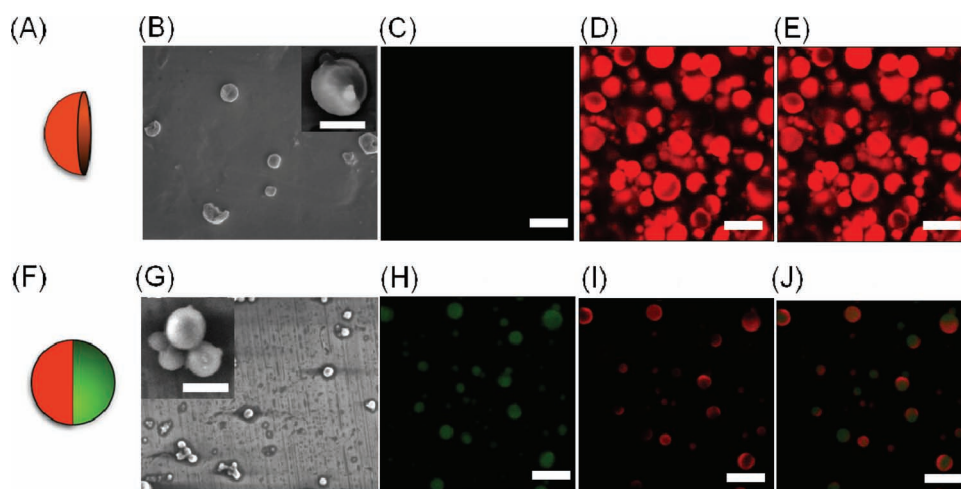


Figure 4. (A, F) Cartoon of the Janus particle shape after storage and degradation at pH 3 versus pH 7. (B) SEM (5.0 kV and 15 000 × magnification) and green (C), red (D) and overlay (E) images obtained by CLSM after incubation of the particles in phosphate buffer (pH 7.4) for 5 days at 37 °C. (G) SEM (5 kV, and 5,000 × magnification) and green (H), red (I) and overlay (J) images obtained by CLSM after incubation of the particles in phosphate buffer (pH 3.0) for 5 days at 37 °C. The scale bars are 1.00 μm in (B) and (G), and 5 μm in (C-E) and (H-J).

pH, the release kinetics was equilibrated at approximately 80% after 5 days, suggesting that a significant alteration of the FITC-PEO release kinetics is associated with the disintegration of the PEO compartment.

Meanwhile, RITC-dextran release (from the second compartment) was negligible under both high and low pH conditions (data not shown) implying that dextran compartment was relatively stable in during the time interval covered in this study. Even though ester hydrolysis at the physiological pH will eventually proceed, this rate is expected to be relatively much lower than the rate of imide. Therefore, all crosslinking junctions are in theory breakable after extended time periods to result full disintegration of the entire particles, a feature that is highly desirable for drug delivery and biocompatibility.

The differential degradation of compartments was further validated by assessing the particle shapes after the degradation experiments. Particles incubated at pH 7.4 took on a hemispherical shape, corresponding to the remaining dextran-containing compartment only (Figure 4A). This is confirmed by the SEM micrograph shown in Figure 4B. Subsequent CLSM analysis unambiguously revealed the absence of any green fluorescence signal from the PEO-containing compartment (Figure 4C), while the red-colored dextran-containing compartment is clearly observable (Figure 4D). In contrast, at pH 3, the particle kept their original shape as depicted in Figure 4F. The SEM picture verified the spherical shape (see Figure 4G), as both compartments were clearly displayed in the CLSM micrographs (see Figure 4H–J; and Figure S2, Supporting Information).

In case of orally administration, those particles likely pass through the stomach with minimizing loss of drug.

Hence, chemically labile drug at a low pH can be orally delivered. After digested, release kinetic profiles of two different drugs in the particles (or one type of drug in two different compartments) can be controlled in a designed manner. The difference to core-shell type particles is that the release profiles from both compartments can be truly decoupled, whereas in the case of core-shell particles, the shell needs to be dissolved first, before drugs located in the core compartment can be released. In principle, one could also consider using mixtures of isotropic particles, each loaded with a different drug. However, in this case, the fate of the particles releasing both drugs is no longer coupled and differently biodistributions may be observed over time; at least to some extent defeating the purpose of coupled release.

4. Conclusion

We have demonstrated bicompartamental polymer particles composed of two different mixtures of polymer hydrogels (one with p(AAm-co-AA) and PEO and the other with the copolymer and dextran) using EHD co-jetting. The combination of physically and chemically crosslinked polymer networks enables decoupled release kinetics for the two compartments. Distinguishable degradation kinetics were clearly observed between the two compartments of the anisotropic particles at physiological pH. In contrast, both compartments were stable at the low pH of the stomach (i.e., pH 3), maintaining their spherical shapes. We note, however, that the herein used crosslinking approach may not be appropriate for many drugs including protein drugs and alternative crosslinking approaches may need to be

developed in these cases. We have demonstrated selective photo-crosslinking of individual compartments in the past and this may offer an alternative in some cases.^[24] Overall, polymers and drugs will have to be selected on a case-to-case basis. The bicompartmental release concept offers the necessary flexibility to accommodate for such changes. Thus, these and similar functionalized anisotropic particles are expected to find potential use for orally administered drugs that must pass the stomach, but should release their cargo at physiological pH. Additionally, this type of multifunctional Janus particles may offer additional value because of the ability to control the pharmacokinetics of multiple drugs leading to complex release profiles.

Supporting Information

Supporting Information is available from the Wiley Online Library or from the authors.

Acknowledgements: The author thanks the American Cancer Society (RSG-08-284-01-CDD) for financial support.

Received: January 26, 2012; Revised: March 3, 2012; Published online: May 18, 2012; DOI:10.1002/marc.201200054

Keywords: colloids; crosslinking; degradation; drug delivery systems; esterification

- [1] J. Lahann, M. Yoshida, *Acs Nano* **2008**, *2*, 1101.
- [2] K. J. Lee, J. Yoon, J. Lahann, *Curr. Opin. Colloid Interface Sci.* **2011**, *16*, 195.
- [3] J. Yoon, K. J. Lee, J. Lahann, *J. Mater. Chem.* **21**, 8502.
- [4] Q. Chen, J. K. Whitmer, S. Jiang, S. C. Bae, E. Luijten, S. Granick, *Science* **2011**, *331*, 199.
- [5] Q. Chen, S. C. Bae, S. Granick, *Nature* **2011**, *469*, 381.
- [6] W. F. Paxton, S. Sundararajan, T. E. Mallouk, A. Sen, *Angew. Chem. Int. Ed.* **2006**, *45*, 5420.
- [7] T. R. Kline, W. F. Paxton, T. E. Mallouk, A. Sen, *Angew. Chem. Int. Ed.* **2005**, *44*, 744.
- [8] M. Yoshida, K. H. Roh, S. Mandal, S. Bhaskar, D. W. Lim, H. Nandivada, X. P. Deng, J. Lahann, *Adv. Mater.* **2009**, *21*, 4920.
- [9] S. H. Kim, A. Abbaspourrad, D. A. Weitz, *J. Am. Chem. Soc.* **2011**, *133*, 5516.
- [10] S. K. Smoukov, S. Gangwal, M. Marquez, O. D. Velev, *Soft Matter* **2009**, *5*, 1285.
- [11] Y. Y. Hong, D. Velegol, N. Chaturvedi, A. Sen, *Phys. Chem. Chem. Phys.* **2010**, *12*, 1423.
- [12] T. Nisisako, T. Torii, T. Takahashi, Y. Takizawa, *Adv. Mater.* **2006**, *18*, 1152.
- [13] S. H. Kim, S. J. Jeon, W. C. Jeong, H. S. Park, S. M. Yang, *Adv. Mater.* **2008**, *20*, 4129.
- [14] N. Doshi, S. Mitragotri, *Adv. Funct. Mater.* **2009**, *19*, 3843.
- [15] J. Choi, Y. H. Zhao, D. Y. Zhang, S. Chien, Y. H. Lo, *Nano Lett.* **2003**, *3*, 995.
- [16] S. C. Chapin, D. C. Appleyard, D. C. Pregibon, P. S. Doyle, *Angew. Chem. Int. Ed.* **2011**, *50*, 2289.
- [17] C. Casagrande, M. Veyssie, *C. R. Acad. Sci. Ser. II* **1988**, *306*, 1423.
- [18] G. Zhang, D. Y. Wang, H. Mohwald, *Angew. Chem. Int. Ed.* **2005**, *44*, 7767.
- [19] D. Dendukuri, D. C. Pregibon, J. Collins, T. A. Hatton, P. S. Doyle, *Nat. Mater.* **2006**, *5*, 365.
- [20] K. H. Roh, D. C. Martin, J. Lahann, *Nat. Mater.* **2005**, *4*, 759.
- [21] K. H. Roh, D. C. Martin, J. Lahann, *J. Am. Chem. Soc.* **2006**, *128*, 6796.
- [22] K. H. Roh, M. Yoshida, J. Lahann, *Langmuir* **2007**, *23*, 5683.
- [23] S. Bhaskar, K. H. Roh, X. W. Jiang, G. L. Baker, J. Lahann, *Macromol. Rapid Commun.* **2008**, *29*, 1655.
- [24] K. J. Lee, S. Hwang, J. Yoon, S. Bhaskar, T. H. Park, J. Lahann, *Macromol. Rapid Commun.* **2011**, *32*, 431.
- [25] S. Hwang, K. H. Roh, D. W. Lim, G. Y. Wang, C. Uher, J. Lahann, *Phys. Chem. Chem. Phys.* **2010**, *12*, 11894.
- [26] D. W. Lim, S. Hwang, O. Uzun, F. Stellacci, J. Lahann, *Macromol. Rapid Commun.* **2010**, *31*, 176.
- [27] M. Liu, C. Xie, H. Pan, J. Pan, W. Y. Lu, *J. Chromatogr. A.* **2006**, *1129*, 61.
- [28] S. Bhaskar, K. M. Pollock, M. Yoshida, J. Lahann, *Small* **2010**, *6*, 404.
- [29] H. Matsuyama, M. Teramoto, K. Matsui, Y. Kitamura, *J. Appl. Polym. Sci.* **2001**, *81*, 936.
- [30] A. Kazemi, J. Lahann, *Small* **2008**, *4*, 1756.
- [31] L. A. Connal, Q. Li, J. F. Quinn, E. Tjipto, F. Caruso, G. G. Qiao, *Macromolecules* **2008**, *41*, 2620.
- [32] W. Z. Hong, W. W. Jiao, J. C. Hu, J. R. Zhang, C. Liu, X. M. Fu, D. Shen, B. Xia, Z. Y. Chang, *J. Biol. Chem.* **2005**, *280*, 27029.